PAN ARCHIVES OF ACOUSTICS
Vol. 43, No. 3, pp. 477–486 (2018)

DOI: 10.24425/123919

Investigations of Auditory Filters Based Excitation Patterns for Assessment of Noise Induced Hearing Loss

Wisam Subhi AL-DAYYENI, Pengfei SUN, Jun QIN

Department of Electrical and Computer Engineering
Mail Code 6603, 1230 Lincoln Drive, Carbondale, IL 62901, USA; e-mail: jqin@siu.edu

(*received July 19, 2017; accepted May 17, 2018*)

Noise induced hearing loss (NIHL) as one of the major avoidable occupational related health issues has been studied for decades. To assess NIHL, the excitation pattern (EP) has been considered as one of the mechanisms to estimate the movements of the basilar membrane (BM) in the cochlea. In this study, two auditory filters, dual resonance nonlinear (DRNL) filter and rounded-exponential (ROEX) filter are applied to create two EPs, the velocity EP and the loudness EP respectively. Two noise hazard metrics are proposed based on two EPs to evaluate hazardous levels caused by different types of noise. Moreover Gaussian noise and single-tone noise are simulated to evaluate performances of the proposed EPs and the noise metrics. The results show that both EPs can reflect the responses of the BM to different types of noise. For Gaussian noise there is a frequency shift between the velocity EP and the loudness EP. The results suggest that both EPs can be used for assessment of NIHL.

Keywords: noise induced hearing loss; excitation pattern; basilar membrane motion; auditory filter; noise assessment metrics.

List of abbreviations

AM – Auditory Model,
BM – Basilar Membrane,
CF – Center Frequency,
DRNL – Dual-Resonance Nonlinear Filter,
EP – Excitation Pattern,
ERB – Equivalent Rectangular Bandwidth,
HL – Hazardous Level,
NIHL – Noise Induced Hearing Loss,
ROEX – Rounded-Exponential filter,
SPL – Sound Pressure Level,
SVTF – Stapes Velocity Transfer Function,
THL – Total Hazard Level.

1. Introduction

Noise-induced hearing loss (NIHL) remains as one of the most common health related problems worldwide. One main cause of NIHL is the exposure to excessive noise (Qin *et al.*, 2014; Rabinowitz, 2000; Wu, Qin, 2013). Approximately, 22 million workers in the United States are exposed to loud noise in workplaces, which are considered at a hazardous level (Tak *et al.*, 2009). Hearing loss has a strong impact on the quality of life; it causes isolation, impairs social interactions, and increases the risk of accidents (Kirchner *et al.*, 2012).

Intrinsically, NIHL can be partially considered as an auditory fatigue phenomenon, in which the motions of stretching and squeezing of the basilar membrane (BM) could damage the hearing cells (i.e., outer and inner hair cells) in the cochlea (Sun *et al.*, 2015; 2017; Sun, Qin, 2016a). The mechanical motions of the BM can be considered as one of the major factors that cause NIHL in the cochlea (Calford *et al.*, 1993; Ohlemiller, 2006). The motions of the BM in response to the noise stimulus as a function of frequency can be stated as an excitation pattern (EP). Therefore, investigations of the EP are very useful for NIHL research (Sun, Qin, 2016b).

An EP represents the distribution of movements along the BM caused by a sound (Fletcher, 1940; Chen *et al.*, 2011). In psychoacoustics, the EP is defined as the output of each auditory filter plotted as a function of the filter's center frequency (CF) (Moore, Glasberg, 1983). The EPs are normally calculated and plotted as the gain of each auditory filter equal to 0 dB at its CF. For example, a tone with a 60 dB SPL and at 1 kHz CF will cause an excitation level equal to 60 dB and at 1 kHz (Zwicker, 1970; Glasberg, Moore, 1990; Chen *et al.*, 2011).

The auditory models (AMs) of the human peripheral frequency selectivity are the fastest ways to esti-

mate the EPs over the BM partitions in the cochlea (Lopez-Poveda, Meddis, 2001). Several AMs have been developed based on observations of input-output behavior of the human auditory system with reference to psychological or physiological responses (Sun *et al.*, 2015). Such AMs include Gammatone filters, dual-resonance nonlinear (DRNL) filters, dynamic-compressive gammachirp filters, etc. Hohmann (2002) developed a 4th-order linear Gammatone filter based AM for speech processing in hearing aids. This linear model can reconstruct acoustical signals in an auditory system, but it does not include nonlinear features (Hohmann, 2002). Lopez-Poveda and Meddis (Lopez-Poveda, Meddis, 2001; Meddis *et al.*, 2001) proposed a nonlinear DRNL filter which successfully simulates the two-tone suppression and the phase responses in the BM. Irino and Patterson (2006) developed a gammachirp filterbank with nonlinear and compressive features. The developed gammachirp filter has a group of linear passive gammachirp filters, and can be used for the applications on speech enhancement, speech coding, and hearing aids (Irino, Patterson, 2006).

Moreover, the AMs can be categorized as mechanical or perceptual model (Saremi *et al.*, 2016). The mechanical AMs are designed to estimate mechanical vibrations on BM in the cochlea (Lopez-Poveda, Meddis, 2001), while the perceptual AMs are developed to mimic the psychoacoustic data (Irino, Patterson, 2006). In this study, a DRNL filter as a typical mechanical AM and a rounded-exponential (ROEX) filter as a typical perceptual AM have been implemented to investigate EPs on the human BM. As a cascade filter model, the DRNL filter was developed to simulate the nonlinear mechanical response of the BM in reaction to stapes motion (Meddis *et al.*, 2001). The output of DRNL filters is the velocity of the BM, which can be described as a velocity EP of the BM in the cochlea. Such velocity EP intuitively can be used to assess the auditory fatigue based NIHL (Sun *et al.*, 2015). On the other hand, the ROEX filter as a perceptual model can be used to demonstrate the loudness levels in the cochlea. Loudness is one of the most important parameters for evaluation of the acoustical quality in various applications, from hearing aid optimizing to automatic music mixing systems (Moore *et al.*, 1997). The loudness estimations directly reflect the characteristics of the human auditory system, such as masking adaption, integration along a perceptual frequency axis, and integration and compression along time axis. In previous studies, loudness contours based models have been developed for evaluations of the annoyance of environment noises, including community noise, industrial noise, and transportation noise (Schomer *et al.*, 2001; Qin *et al.*, 2014; Sun *et al.*, 2016).

In this study, we implement the DRNL filter and the ROEX filter to create two EPs, the velocity EP and the loudness EP, respectively. To evaluate the performances of the proposed EPs, Gaussian noise and single-tone noise with various parameters (e.g. amplitude and frequency) are simulated. In addition, two noise metrics are proposed based on two proposed EPs to estimate the hazardous levels caused by different types of noise. The rest of this paper is organized as follows: Sec. 2 describes the auditory filters, the proposed noise metrics, and simulations of noise signals; Sec. 3 gives results and discussions; Sec. 4 concludes the paper and outlines future works.

2. Material and methods

2.1. Transfer functions of external ear and middle ear

The transfer functions of the external ear used for both the DRNL filter and the ROEX filter are the same in this study. As shown in Fig. 1, the transfer function of the external ear was described in Moore's work (Moore *et al.*, 1997) and ANSI-S3-2007 (ANSI, 2007).

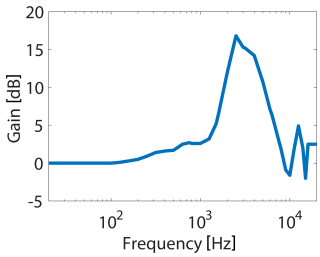

Fig. 1. Frequency response of the transfer function of the external ear.

In this study, two different transfer functions of the middle ear are used for the DRNL filter and the ROEX filter, respectively. Figure 2a shows the transfer function of the middle ear used for the DRNL filter as described in Meddis's work (Meddis *et al.*, 2001), in which the acoustical pressure is converted into the stapes velocity, called the stapes velocity transfer function (SVTF). For the ROEX filter, the transfer function of the middle ear that is used in the procedure of loudness computation is based on Moore's work

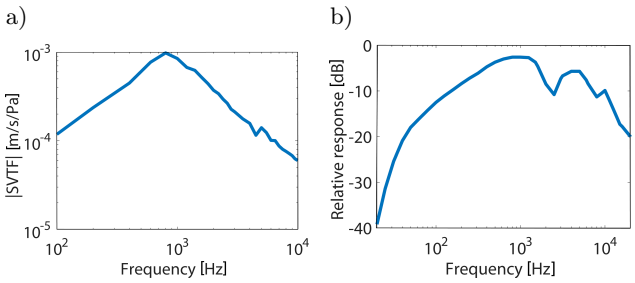

Fig. 2. Frequency responses of the transfer function of the middle ear, which are applied to (a) the DRNL filter and (b) the ROEX filter, respectively.

(Moore *et al.*, 1997). Figure 2b shows the transfer function used for the ROEX filter.

2.2. DRNL filter

A DRNL filter is utilized to obtain the BM movements in the human cochlea (Meddis *et al.*, 2001). The DRNL filter simulates the velocity of BM as a response to the stapes velocity in the middle ear. As shown in Fig. 3, the input of the DRNL filter is the linear stapes velocity. Each individual site is represented as a tuned system with two parallel independent paths, one linear (right) and one nonlinear (left). The linear path consists of a gain/attenuation factor, a bandpass function, and a low pass function in a cascade. The nonlinear path is a cascade combination of the 1st bandpass function, a compression function, the 2nd bandpass function, and a low pass function. The output of the DRNL filter is the sum of the outputs of the linear and nonlinear paths, and is the BM velocity at a particular location along the cochlear partition.

In both paths, each of the three bandpass functions consists of a cascade of two or three 1st order Gammatone filters (Hartmann, 1997) with a unit gain at the center frequency. Two low-pass functions are the same and consist of a cascade of four 2nd order Butterworth low pass filters.

Moreover, the compression function in the nonlinear path was defined based on the animal data, and it can be described as (Meddis *et al.*, 2001)

$$y[t] = \text{sign}(x[t]) \cdot \min(a|x[t]|, b|x[t]|^c), \qquad (1)$$

where $x[t]$ represents the output from the first bandpass function in the nonlinear path; a, b and c are the model parameters as summarized in Table 1.

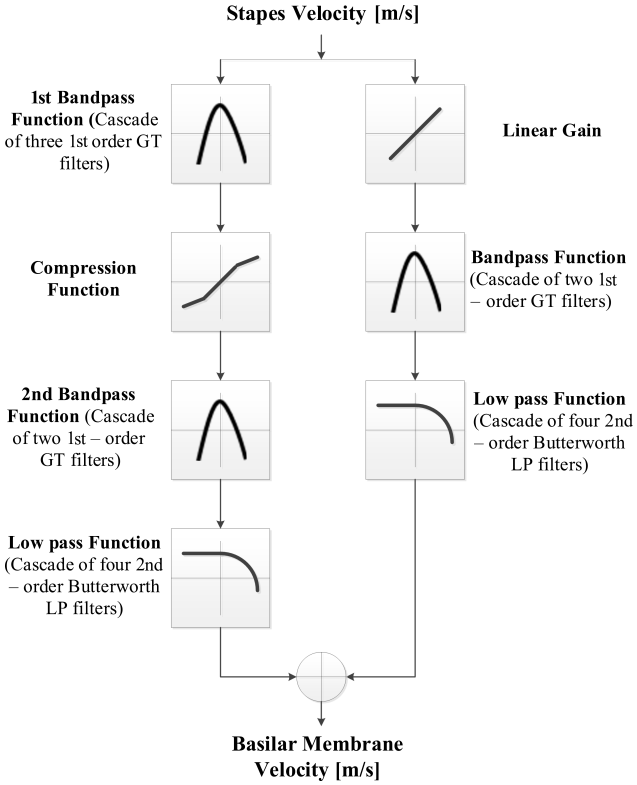

Fig. 3. Schematic diagram of the DRNL filter in which the velocities of stapes in the middle ear are passed through two parallel branches to obtain the velocities of BM.

Table 1 summarizes the parameters of the DRNL filter for human which was used to implement the DRNL filter in this study. The velocity EP is the distribution of BM velocity which can be obtained as the outputs of the DRNL filter.

Table 1. DRNL filter parameters used to simulate the human inner ear (Lopez-Poveda, Meddis, 2001).

Simulated preparation	0.25 kHz	0.5 kHz	1 kHz	2 kHz	4 kHz	8 kHz
Linear						
GT cascade	2	2	2	2	2	2
LP cascade	4	4	4	4	4	4
CF_{lin}	235	460	945	1895	3900	7450
BW_{lin}	115	150	240	390	620	1550
LP_{lin}	235	460	945	1895	3900	7450
Gain, g	1400	800	520	400	270	250
Nonlinear						
GT cascade	3	3	3	3	3	3
LP cascade	3	3	3	3	3	3
CF_{lin}	250	500	1000	2000	4000	8000
BW_{lin}	84	103	175	300	560	1100
LP_{nl}	250	500	1000	2000	4000	8000
Gain, a	2124	4609	4598	9244	30274	76354
Gain, b	0.45	0.28	0.13	0.078	0.06	0.035
Exponent, c	0.25	0.25	0.25	0.25	0.25	0.25

2.3. ROEX filter

The ROEX filter was originally derived from psychophysical data (Patterson, 1976). It is a descriptive model which presents the shape of the transfer function of an auditory filter (Patterson, 1976). The ROEX filter formula can be defined by (ANSI, 2007)

$$W(g) = (1 + pg) \exp(-pg), \tag{2}$$

where g is the normalized deviation from the center frequency (CF) divided by the CF, and p is an adjustable parameter which determines the slope and the bandwidth of the filter.

In this study the ROEX filter is implemented according to ANSI 3.4-2005 (ANSI, 2005). To calculate the input level at each Equivalent Rectangular Bandwidth (ERB), p in Eq. (2) is set to be $4f/\text{ERB}$. The ERB is a psychoacoustic measurement of the width of the auditory filter in each location along the cochlea, and it can be defined as (ANSI, 2007)

$$\text{ERB} = 24.673\,(0.004368 f_c + 1), \tag{3}$$

where f_c is the CF in Hz, which are in the range of 50 Hz – 15 kHz in this study. The ERB is obtained according to the input level which is used to determine the ROEX filter shape. The energy in each ERB can be obtained by (Sun, Qin, 2016b)

$$E_i = \frac{\sum W(g_{i,j})\, P_j^2}{P_0^2} E_0, \tag{4}$$

where W represents local ROEX filter in the i-th ERB. P_j^2 refers to the power in the j-th frequency band. E_0 is the reference energy at 1 kHz CF and 0 dB SPL, and P_0 is the reference pressure referring to $2 \cdot 10^{-5}$ Pa. For the selected frequencies, E_i will be transformed to loudness levels according to the values of the excitation threshold (ANSI, 2007)

$$N = C\left[(GE + 2E_{\text{THRQ}})^{\alpha} - (2E_{\text{THRQ}})^{\alpha}\right], \tag{5}$$

where E is the energy, and G is the low level gain. C and α are two constants, where $C = 0.046871$, and α is related to the G value. E_{THRQ} refers to lower threshold of human perception.

Figure 4 shows the shape of the ROEX filter at 0.5, 1, 2, 4, and 8 kHz center frequencies when the levels change from 10 to 100 dB in 10-dB steps. The ROEX filter is a dynamic filter which has different frequency gains when the sound pressure level (SPL) changes. As the SPL level increases the curve of the ROEX filter becomes more flat. In general, when the SPL increases, there will be more energy passed through the ROEX filter. From this perspective, the ROEX filter is consistent with the loudness contours. When SPLs increase, loudness contours become flat (Moore, Glasberg, 1983; ANSI, 2007).

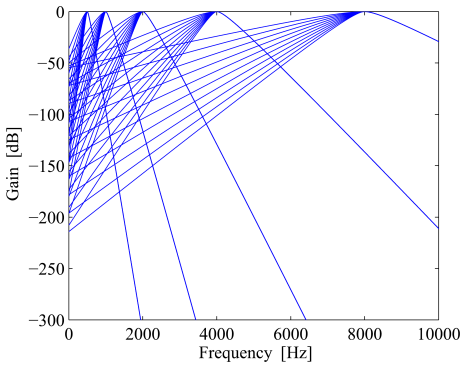

Fig. 4. Shape of the ROEX filter centered at 0.5, 1, 2, 4, and 8 kHz for levels from 10 dB to 100 dB with 10-dB step.

2.4. EP based noise metrics

Previous studies have demonstrated that the EPs of the BM are highly correlated with NIHL in the human cochlea (Crane, 1966; Sun *et al.*, 2015; Sun, Qin, 2016b). To investigate hearing loss two EPs based metrics are proposed to assess the potential hazardous levels (HLs) caused by different types of noise. Since the EP represents the temporal responses of the organ of Corti in the cochlea, one can integrate the local responses and obtains the cumulative HLs. Therefore two proposed noise metrics HL_i^D and HL_i^R can be defined as (Sun, Qin, 2016b)

$$\text{HL}_i^D = 10 \log_{10} \sum_{t=1}^{t=n} \frac{V(i,t)^2}{V_o^2}, \tag{6}$$

$$\text{HL}_i^R = 10 \log_{10} \sum_{t=1}^{t=n} \frac{N(i,t)^2}{N_o^2}, \tag{7}$$

where HL_i^D represents the hazard level based on the velocity EP, and $V(i,t)$ refers to the BM velocity at the i-th frequency of BM at a time t. V_0 represents the BM velocity located at the CF equal to 1 kHz. Moreover, HL_i^R represents the hazard level based on the loudness EP, and $N(i,t)$ refers to the loudness level at the i-th frequency of BM at a time t. N_0 is the loudness level at CF equal to 1 kHz. By Eq. (6) and Eq. (7), the developed EPs have been successfully translated to the amount of HLs, which can be used for the assessment of NIHL.

Moreover, total hazard level (THL) can be defined as summation of HLs:

$$\text{THL}^D = \sum_i \text{HL}_i^D, \tag{8}$$

$$\text{THL}^R = \sum_i \text{HL}_i^R, \tag{9}$$

where THL^D and THL^R represent THLs based on the velocity EP and the loudness EP, respectively.

2.5. Simulation of noise signals

In this study, two different types of noise signals (i.e., Gaussian noise and single-tone noise) have been simulated to evaluate the performances of the two proposed EPs. The Gaussian noise signals are simulated using the "randn" function in MATLAB, in which the probability distribution function of the Gaussian noise is given by (Hussain *et al.*, 2011):

$$P(t) = \frac{1}{\sigma\sqrt{2\pi}} \exp\left[-\frac{(t-\mu)^2}{2\sigma^2}\right], \tag{10}$$

where μ is the mean, and σ is the standard deviation. μ is equal to zero in this study.

The single-tone signal in this study is given by:

$$y(t) = A\cos 2\pi f t, \tag{11}$$

where A is the amplitude of the signal, and f is the frequency.

3. Results and discussion

3.1. Time-Frequency (T-F) representations of two EPs

In this section, the simulated Gaussian noise and single-tone noise signals are fed into the DRNL filter and the ROEX filter to obtain the proposed velocity EP and loudness EP, respectively. Both EPs can be represented in the joint time and frequency (T-F) domain. Figures 5a and 5b show the T-F representations of the velocity EP and the loudness EP responding to a simulated Gaussian noise at 100 dB SPL respectively.

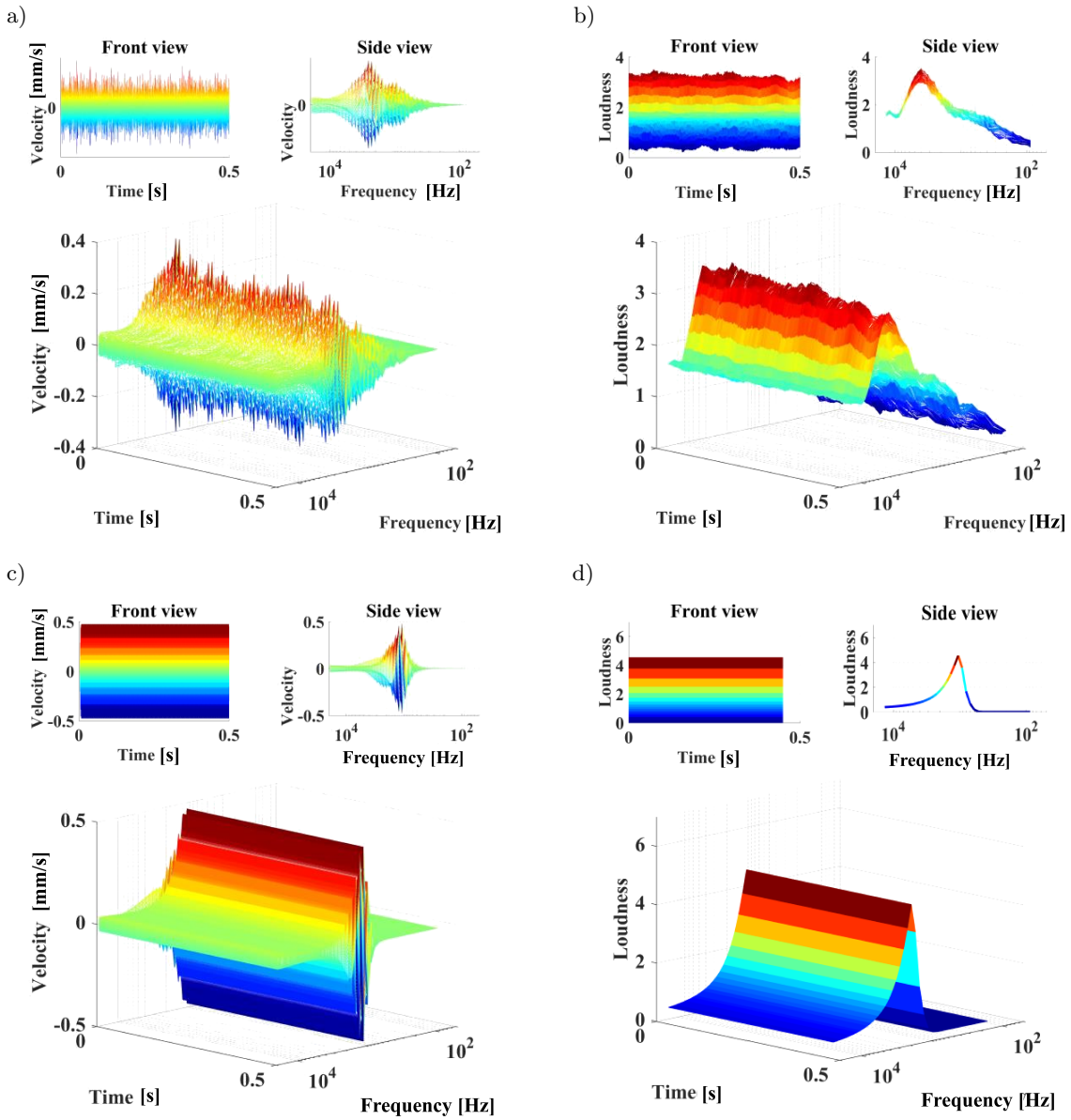

Fig. 5. T-F representations of (a) the velocity EP and (b) the loudness EP responding to a Gaussian noise at 100 dB SPL, and (c) the velocity EP and (d) the loudness EP with respect to a single-tone noise at 100 dB SPL and 1 kHz.

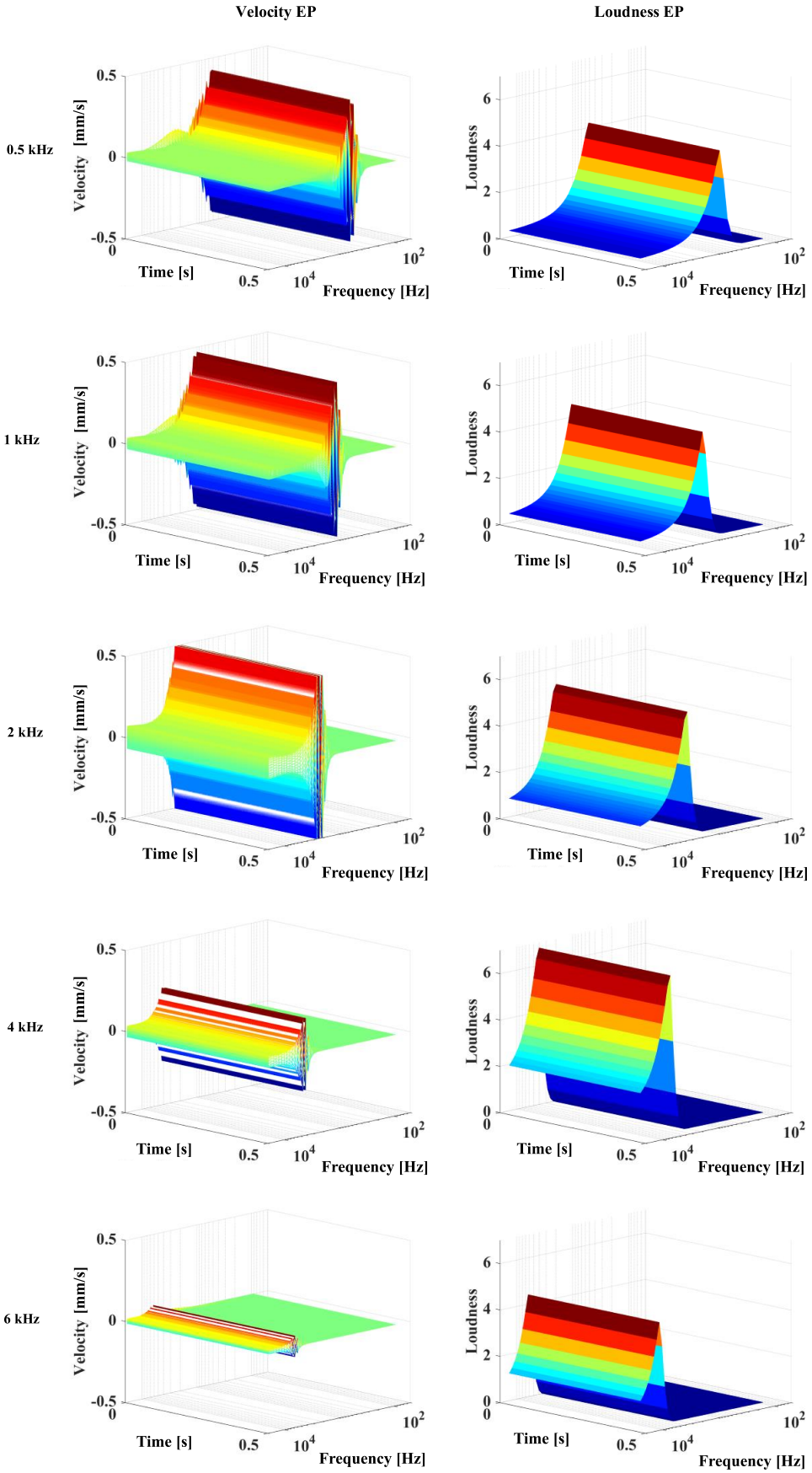

Fig. 6. T-F distributions of two proposed EPs obtained by simulated single-tone noise signals at 100 dB SPL with frequencies at 0.5, 1, 2, 4, and 6 kHz, respectively.

Figures 5c and 5d show the T-F representations of the velocity EP and the loudness EP responding to a single-tone noise with 100 dB SPL and 1 kHz frequency respectively. The results show that both EPs can reflect the amplitudes and transitions of the noise signals. The velocity EP as a mechanical model can characterize both positive and negative vibrations of BM in the cochlea which reflects more realistic representations of the stretching and squeezing on the hair cells in the cochlea. On the other hand the loudness EP as a perceptual model can only represent the positive amount of the loudness as a response to the noise signal. The loudness EP doesn't directly reflect the BM vibrations in the cochlea.

Moreover, along the time axis, the velocity EP presents higher temporal resolution than the loudness EP for Gaussian noise. It indicates that the temporal resolution of the DRNL filter is better than the ROEX filter. Along the frequency axis, for the Gaussian noise, the peak frequency of the velocity EP is around 2 kHz and is lower than the corresponding value of the loudness EP which is around 4 kHz. For the single-tone noise, both EPs present the peak frequencies at 1 kHz, which reflects the frequency of the input tone signal. However, the velocity EP shows vibrations around 1 kHz since it reflects the BM motion while the loudness EP shows only one pulse since it is a perceptual model that reflects the amount of psychoacoustic data.

3.2. T-F representations of two EPs for single-tone noise

Figure 6 shows the T-F representations of the velocity EP and the loudness EP produced by single-tone signals with 100 dB SPL at various frequencies equal to 0.5, 1, 2, 4, and 6 kHz. For the velocity EP (as shown in the left side of Fig. 6), the amplitudes have both positive and negative values, which reflects the BM vibrations. Moreover, all the velocity EPs peak at CF similar to the frequency of the input signals. It can also be found that the peaks of the velocity EPs are decreasing with the frequency higher than 2 kHz because of the bandpass filtering effects in the middle ear. Furthermore, the loudness EP (as shown in the right side of Fig. 6) presents only positive amplitudes, and the peaks match the frequencies of the stimulated single-tone signals. The peaks of the loudness EP increase first and then decrease with the frequency increasing, and the maximum peak amplitude appears at 4 kHz.

3.3. Hazardous level evaluation

3.3.1. Frequency distributions of HLs for Gaussian noise

The performances of the two EPs are evaluated using the two proposed metrics (i.e., HL_i^D and HL_i^R) which are used to depict HL at the frequency locations on the BM. Figure 7 shows the frequency distributions of the normalized HLs generated by the simulated Gaussian noise signals at SPL range from 70 to 120 dB with 10 dB interval. For both velocity EP and loudness EP, the HLs rise with SPL increase. Overall, the loudness EP shows broader frequency response compared with the velocity EP. The results also show that there is a frequency shift between the two EPs. The peak HLs of the velocity EP are around 2 kHz, while the peak HLs of the loudness EP are around 4 kHz. Since the BM motions are associated with hearing loss in the cochlea, the peak frequency shift between the two EPs indicates that the maximum hearing loss predicted by these two EPs may occur at different partitions of BM.

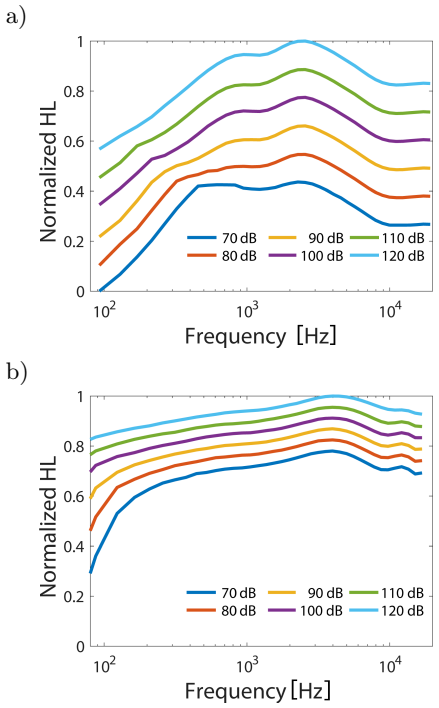

Fig. 7. Frequency distributions of normalized HLs based on (a) the velocity EP and (b) the loudness EP generated by simulated Gaussian noise signals at SPL = 70 to 120 dB with 10 dB interval.

3.3.2. Frequency distributions of HLs for single-tone noise

Figure 8 shows the normalized HLs generated by simulated single-tone signals at 1 kHz and SPL range from 70 to 120 dB with 10 dB interval. Both the velocity EP and the loudness EP show the peak frequency responses at 1 kHz, which is same as the frequency of the input single-tone signals. It can be found that the HLs are rising with SPL levels increasing in both EPs. As shown in Fig. 8a, the HLs of the velocity EP gradually increase when the frequency is smaller than 1 kHz, and then gradually decrease after the frequency is greater than 1 kHz. Comparatively, as shown in Fig. 8b, the HLs of the loudness EP show different

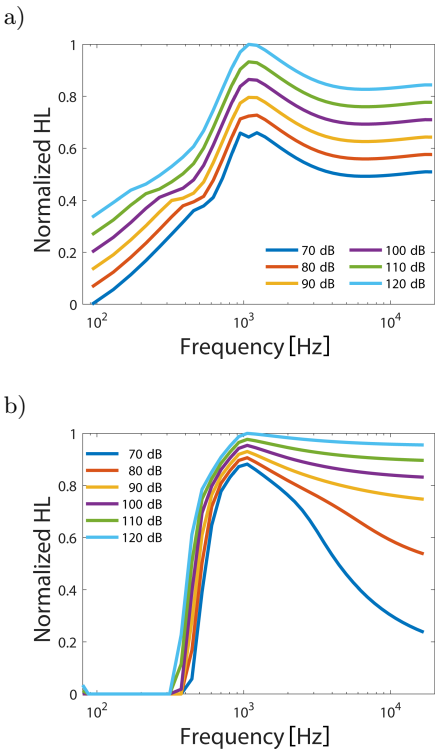

Fig. 8. Frequency distributions of normalized hazardous levels based on (a) the velocity EP and (b) the loudness EP, obtained at 1 kHz tone and SPL = 70 to 120 dB with 10 dB interval.

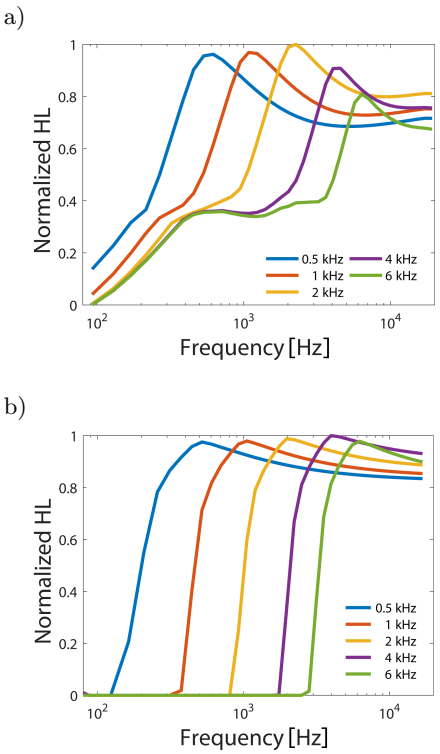

Fig. 9. Frequency distributions of normalized hazardous levels based on (a) the velocity EP and (b) the loudness EP, obtained at various frequencies (0.5, 1, 2, 4, and 6 kHz) with fixed SPL = 100 dB.

frequency responses than the velocity EP. The HLs of the loudness EP almost equal to zero when frequency is smaller than 500 Hz, and then rapidly increase to reach the peak at 1 kHz, and finally gradually decrease after 1 kHz. This is because the loudness EP is based on the ROEX filter which is derived from psychophysical data. Therefore the loudness EP may not reflect the real motion of the BM in the cochlea.

Moreover, Fig. 9 shows the normalized HLs generated by the simulated single-tone signals at different frequencies (0.5, 1, 2, 4, and 6 kHz) with SPL equal to 100 dB. Both velocity EP and loudness EP can reflect the corresponding frequencies of the input tone signals. The peak HLs of the velocity EP (as shown in Fig. 9a) are reducing after the frequency larger than 2 kHz, while the peak HLs of the loudness EP slightly reduce when the frequency is higher than 4 kHz. In the velocity EP, the maximum velocity occurs around 2 kHz, while in the loudness EP, the maximum loudness appears around 4 kHz.

3.3.3. Total hazardous levels for Gaussian noise

The total hazardous levels (i.e., THL^D and THL^R) can be calculated based on the velocity EP and the loudness EP, respectively. THLs can be used to assess the hazard level of high noise exposure, and can be used to investigate NIHL. Figure 10 shows the normalized THLs for the Gaussian noise at SPL from 70 to 120 dB. The result shows that THLs of both EPs are increasing with SPL increasing. The increasing rate of the velocity EP is faster than that of the loudness EP. Compared with the loudness EP, the velocity EP shows lower THLs at SPL $<$ 100 dB, but demonstrates higher THLs when SPL $>$ 100 dB.

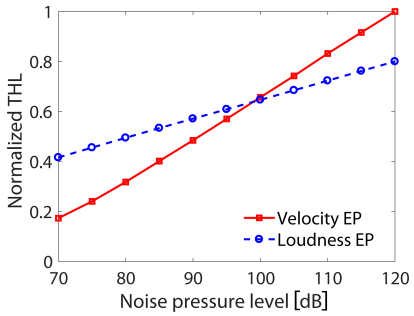

Fig. 10. Normalized THLs for the Gaussian noise at SPL from 70 to 120 dB for the velocity EP and the loudness EP.

3.3.4. THLs for single-tone noise

Figure 11a shows the normalized THLs of both EPs produced by the simulated single-tone signals with increasing SPL from 70 to 120 dB and fixed frequency at 1 kHz. The THLs of both EPs are rising with SPL increasing. Specifically, the velocity EP increases faster than the loudness EP. The result indicates that the velocity EP is more sensitive with SPL increasing than

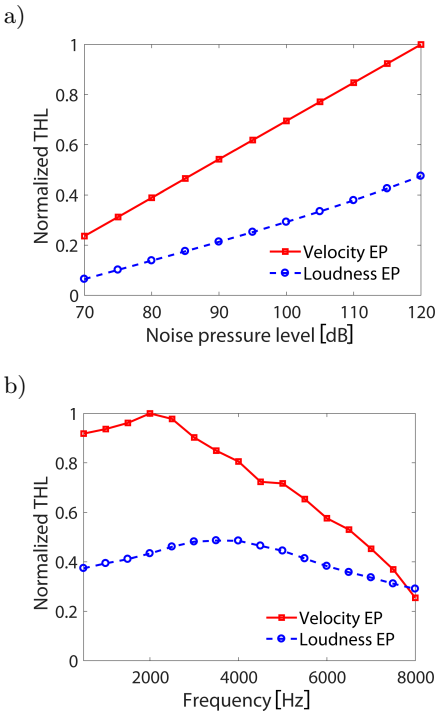

Fig. 11. Normalized THLs for the single-tone noise: (a) at 1 kHz and SPL from 70 to 120 dB, and (b) at fixed SPL = 100 dB and frequencies from 0.5 to 8 kHz for the velocity EP and the loudness EP.

the loudness EP. It can also be found that the THLs of the velocity EP are constantly higher than the corresponding values of the loudness.

Figure 11b shows the normalized THLs of both EPs generated by the simulated single-tone signals at SPL equal to 100 dB with various frequencies from 0.5 to 8 kHz. For both EPs, the THLs increase first and then decrease with the frequency increasing. The peak THL of the velocity EP is at 2 kHz, while the THL of the loudness EP peaks at 4 kHz. In addition, the velocity EP shows a fast degradation of THL when the frequency increases more than 2 kHz.

4. Conclusions

In this study, two auditory filters (i.e., the DRNL filter and the ROEX filter) have been applied to develop the velocity EP and the loudness EP, respectively. Two different types of noise (i.e., Gaussian noise and single-tone noise) have been simulated to evaluate the two proposed EPs. For Gaussian noise, the results show that the maximum velocity obtained by the DRNL filter occurs around 2 kHz, while the peak loudness obtained by the ROEX filter is about 4 kHz. For single-tone noise, both EPs can accurately reflect the frequencies of the input noise signals. To evaluate the effectiveness of two EPs for the prediction of NIHL, we proposed two noise metrics, HL^D and HL^R, based on the velocity EP and the loudness EP, respectively. The results show that both EPs can be used as noise hazardous level index for assessment of NIHL. The velocity EP based metric demonstrates higher sensitivity than the loudness EP based metric. However, because the current study is only based on theoretical analysis and simulated noise signals, it may be limited to evaluate the performance of two auditory filters. In our future work, we will utilize experimental animal and human noise exposure data to evaluate the developed velocity EP and loudness EP for assessment of NIHL.

References

1. ANSI (2005), *American National Standard: procedure for the computation of loudness of steady sounds*, Melville, N.Y.: Standards Secretariat, Acoustical Society of America.
2. ANSI (2007), *Procedure for the computation of loudness of steady sounds*, ANSI S3, 4-2007.
3. Calford M., Rajan R., Irvine D. (1993), *Rapid changes in the frequency tuning of neurons in cat auditory cortex resulting from pure-tone-induced temporary threshold shift*, Neuroscience, **55**, 4, 953–964.
4. Chen Z., HuG., Glasberg, B.R., Moore B.C. (2011), *A new method of calculating auditory excitation patterns and loudness for steady sounds,* Hearing research, **282**, 1, 204–215.
5. Crane H. (1966), *Mechanical impact: a model for auditory excitation and fatigue*. The Journal of the Acoustical Society of America, **40**, 5, 1147–1159.
6. Fletcher H. (1940), *Auditory patterns*, Reviews of Modern Physics, **12**, 1, 47.
7. Glasberg B.R., Moore B.C. (1990), *Derivation of auditory filter shapes from notched-noise data,* Hearing Research, **47**, 1–2, 103–138.
8. Hartmann W.M. (1997), *Signals, sound, and sensation*, Springer Science & Business Media.
9. Hohmann V. (2002), *Frequency analysis and synthesis using a Gammatone filterbank,* Acta Acustica united with Acustica, **88**, 3, 433–442.
10. Hussain Z.M., Sadik A.Z., O'Shea P. (2011), *Digital signal processing: an introduction with MATLAB and applications*, Springer Science & Business Media.
11. Irino T., Patterson R.D. (2006), *A dynamic compressive gammachirp auditory filterbank,* Audio, Speech, and Language Processing, IEEE Transactions on, **14**, 6, 2222–2232.
12. Kirchner D.B. *et al.* (2012), *Occupational noise-induced hearing loss: ACOEM Task Force on occupational hearing loss*, Journal of Occupational and Environmental Medicine, **54**, 1, 106–108.
13. Lopez-Poveda E.A., Meddis R. (2001), *A human nonlinear cochlear filterbank,* The Journal of the Acoustical Society of America, **110**, 6, 3107–3118.
14. Meddis R., O'Mard L., Lopez-Poveda E.A. (2001), *A computational algorithm for computing nonlinear auditory frequency selectivity* The Journal of the Acoustical Society of America, **109**, 6, 2852–2861.

15. Moore B.C., Glasberg B.R. (1983), *Suggested formulae for calculating auditory-filter bandwidths and excitation patterns*, The Journal of the Acoustical Society of America, **74**, 3, 750–753.

16. Moore B.C., Glasberg B.R., Baer T. (1997), *A model for the prediction of thresholds, loudness, and partial loudness*, Journal of the Audio Engineering Society, **45**, 4, 224–240.

17. Ohlemiller K.K. (2006), *Contributions of mouse models to understanding of age-and noise-related hearing loss*, Brain Research, **1091**, 1, 89–102.

18. Patterson R.D. (1976), *Auditory filter shapes derived with noise stimuli*, The Journal of the Acoustical Society of America, **59**, 3, 640–654.

19. Qin J., Jiang Y., Mahdi A. (2014), *Recent developments on noise induced hearing loss for military and industrial applications*, Biosensors Journal, **3**, e101.

20. Qin J., Sun P., Walker J. (2014), *Measurement of field complex noise using a novel acoustic detection system*, Paper presented at the AUTOTESTCON 2014, IEEE.

21. Rabinowitz P.M. (2000), *Noise-induced hearing loss,* American Family Physician, **61**, 9, 2759–2760.

22. Saremi A., Beutelmann R., Dietz M., Ashida G., Kretzberg J., Verhulst S. (2016), *A comparative study of seven human cochlear filter models*, The Journal of the Acoustical Society of America, **140**, 3, 1618–1634.

23. Schomer P.D., Suzuki Y., Saito F. (2001), *Evaluation of loudness-level weightings for assessing the annoyance of environmental noise*, The Journal of the Acoustical Society of America, **110**, 5, 2390–2397.

24. Sun P., Fox D., Campbell K., Qin J. (2017), *Auditory fatigue model applications to predict noise induced hearing loss in human and chinchilla*, Applied Acoustics, **119**, 57–65.

25. Sun P., Qin J. (2016a), *Auditory fatigue models for prediction of gradually developed noise induced hearing loss*, Paper presented at the 2016 IEEE-EMBS International Conference on Biomedical and Health Informatics (BHI).

26. Sun P., Qin J. (2016b), *Excitation patterns of two auditory models applied for noise induced hearing loss assessment*, Paper presented at the 2016 IEEE-EMBS International Conference on Biomedical and Health Informatics (BHI).

27. Sun P., Qin J., Campbell K. (2015), *Fatigue Modeling via Mammalian Auditory System for prediction of noise induced hearing loss*, Computational and Mathematical Methods in Medicine, **2015**, Article ID 753864, 13 pages, http://dx.doi.org/10.1155/2015/753864.

28. Sun P., Qin J., Qiu W. (2016), *Development and validation of a new adaptive weighting for auditory risk assessment of complex noise*, Applied Acoustics, **103**, 30–36.

29. Tak S., Davis R.R., Calvert G.M. (2009), *Exposure to hazardous workplace noise and use of hearing protection devices among US workers—NHANES, 1999–2004*, American Journal of Industrial Medicine, **52**, 5, 358–371.

30. Wu Q., Qin J. (2013), *Effects of key parameters of impulse noise on prediction of the auditory hazard using AHAAH model*, International Journal of Computational Biology ond Drug Design, **6**, 3, 210–220.

31. Zwicker E. (1970), *Masking and psychological excitation as consequences of the ear's frequency analysis*, [in:] *Frequency Analysis and Periodicity Detection in Hearing*, R. Plomp, G.F. Smoorenburg [Eds.], pp. 376–394, Sijthoff, Leiden.